Space Weather

RESEARCH ARTICLE
10.1029/2019SW002250

Special Section:
Scientific Challenges of Space Weather Forecasting Including Extremes

Intensity and Impact of the New York Railroad Superstorm of May 1921

Jeffrey J. Love[1], Hisashi Hayakawa[2,3], and Edward W. Cliver[4]

[1]Geomagnetism Program, U.S. Geological Survey, Denver, CO, USA, [2]Graduate School of Letters, Osaka University, Toyonaka, Japan, [3]Science and Technology Facilities Council, RAL Space, Rutherford Appleton Laboratory, Didcot, UK, [4]National Solar Observatory, Boulder, CO, USA

Key Points:
- The magnetic storm of May 1921 attained a maximum $-Dst$ of 907 ± 132 nT
- Low-latitude geomagnetic disturbance exhibited extreme local time asymmetry
- Anecdotal evidence from impacts across New York State underscores importance of recent research on geomagnetically induced currents

Supporting Information:
- Supporting information S1

Correspondence to:
J. J. Love,
jlove@usgs.gov

Citation:
Love, J. J., Hayakawa, H., & Cliver, E. W. (2019). Intensity and impact of the New York Railroad superstorm of May 1921. *Space Weather*, *17*, 1281–1292. https://doi.org/10.1029/2019SW002250

Received 18 MAY 2019
Accepted 8 JUL 2019
Accepted article online 16 JUL 2019
Published online 22 AUG 2019

Abstract Analysis is made of low-latitude ground-based magnetometer data recording the magnetic superstorm of May 1921. By inference, the storm was driven by a series of interplanetary coronal mass ejections, one of which produced a maximum pressure on the magnetopause of ~64.5 nPa, sufficient to compress the subsolar magnetopause radius to ~5.3 Earth radii. Over the course of the storm, low-latitude geomagnetic disturbance exhibited extreme local time (longitude) asymmetry that can be attributed to substorm disturbance extending to low latitudes. The storm attained an estimated maximum $-Dst$ on 15 May of 907 ± 132 nT, an intensity comparable to that of the Carrington event of 1859. The May 1921 storm brought spectacular aurorae to the nighttime sky. It also interfered with and damaged telephone and telegraph systems associated with railroad systems in New York City and State. These later effects were due to a combination of three factors: the localized details of geomagnetic vector disturbance, the geographic expression of the Earth's surface impedance tensor, and the configurations and physical parameters of the electrical networks of the day.

Plain Language Summary Historical records of ground-level geomagnetic disturbance are analyzed for the magnetic superstorm of May 1921. This storm was almost certainly driven by a series of interplanetary coronal mass ejections of plasma from an active region on the Sun. The May 1921 storm was one of the most intense ever recorded by ground-level magnetometers. It exhibited violent levels of geomagnetic disturbance, caused widespread interference to telephone and telegraph systems in New York City and State, and brought spectacular aurorae to the nighttime sky. Results inform modern projects for assessing and mitigating the effects of magnetic storms that might occur in the future.

1. Introduction

The storm time disturbance index known as *Dst* is important for identifying the various evolutionary phases of individual magnetic storms (e.g., Loewe & Prölss, 1997; McPherron, 1995) and for studying the long-term statistical occurrence rate of storms, especially extremely intense storms (e.g., Echer et al., 2011; Love et al., 2015; Riley, 2018). It is calculated by averaging disturbance in horizontal-component geomagnetic field measurements from low-latitude ground-based observatories (Sugiura, 1964). During quiet space weather conditions, $Dst \approx 0$ nT, but during the main phase of a magnetic storm, intensification of the westward-directed magnetospheric ring current (e.g., Daglis, 2001) causes a proportional decrease in low-latitude geomagnetic field intensity, and *Dst* takes on negative values (e.g., Gonzalez et al., 1994). An intense storm can attain a maximum $-Dst$ of several hundred nanoteslas. The standard version of *Dst* is calculated using magnetometer data from four low-latitude magnetic observatories (widely separated in longitude; Sugiura & Kamei, 1991). It is continuous in time from 1957 to the present.

Estimating *Dst* for great storms prior to 1957 is challenging because of the relative sparsity of observatories and limited dynamic range in many analog magnetogram recording systems. For example, estimates of storm maximum intensity of the Carrington superstorm of 1859, $-Dst \approx 850$ nT (Siscoe et al., 2006) and $-Dst \approx 1{,}050$ nT (Gonzalez et al., 2011), are based on geomagnetic field measurements from a single low-latitude observatory (Tsurutani et al., 2003)—other low-latitude records are incomplete. This means that the intensity of the Carrington event is very uncertain, making it difficult to compare with well-recorded storms. The superstorm of May 1921 (e.g.,Kappenman, 2006; Silverman & Cliver, 2001) is sometimes called the "New York Railroad Storm" (e.g., Hapgood, 2018a; Jonas et al., 2018; Riswadkar & Dobbins, 2010; Vennerstrom et al., 2016)

because of the disruption it brought to telegraph systems associated with railroads operated in New York City and State. The May 1921 storm might have had an intensity rivaling that of the Carrington event, but the accuracy of its estimated maximum −*Dst* (Kappenman, 2006) has been (to date) uncertain because, like the Carrington event, estimates have been based on measurements from just a single low-latitude observatory.

As part of an ongoing project to obtain improved estimates of the intensities of past magnetic storms (Cliver & Dietrich, 2013; Hayakawa, Mitsuma, et al., 2017; Hayakawa, Tamazawa, et al., 2017; Hayakawa, Ebihara, Hand, et al., 2018; Hayakawa, Ebihara, Willis, et al., 2018; Love, 2018; Love, Hayakawa, & Cliver, 2019), we examine historical magnetic observatory recordings of the May 1921 storm in order to estimate its *Dst* time series. We have identified magnetograms of reasonable completeness from four low-latitude observatories suitable for obtaining an accurate estimate of the *Dst* time series for the May 1921 storm. Results provide new insight into the nature of magnetic superstorms (e.g., Ganushkina et al., 2017; Lakhina & Tsurutani, 2018) and the impacts that they might carry for modern technological systems (e.g., Baker et al., 2008; Cannon et al., 2013; Eastwood et al., 2017; Schieb & Gibson, 2011). This research is consistent with priorities established by the U.S. National Science and Technology Council (2015, 2019) and allied international organizations (Schrijver et al., 2015).

2. The Standard *Dst* Time Series

The standard version of *Dst* is produced by the World Data Center for Geomagnetism, Kyoto (Sugiura & Kamei, 1991; World Data Center for Geomagnetism, Kyoto, 2015). It is continuous in time since the International Geophysical Year (IGY, 1957–1958), when the index was introduced and when improvements were brought to observatory operations and data reporting (Various, 1957; Wienert, 1970). The Kyoto *Dst* has 1-hr resolution and is calculated from data from observatories at Hermanus (HER), South Africa (Kotzé, 2018); Kakioka (KAK), Japan (Minamoto, 2013); Honolulu (HON), Hawaii; and San Juan (SJG), Puerto Rico (Love & Finn, 2011). Since the 1980s, data from these and other observatories around the world have been acquired with digital electronic magnetometer systems (e.g., Newitt, 2007). Today, most magnetic observatory agencies (e.g., Love, 2008) cooperate through and contribute data to INTERMAGNET, a consortium that promotes the operation of observatories according to modern standards (e.g., Love & Chulliat, 2013).

Prior to the development and deployment of digital acquisition systems, continuous monitoring of the Earth's magnetic field was accomplished at observatories with photographic self-registering analog systems (e.g., Schröder & Wiederkehr, 2000). The product of these systems was paper magnetogram records of the vector components of geomagnetic field variation. Typically, these magnetograms were 1 day in length, with time resolution of a few minutes, and time-stamp accuracy of about 10 min. Measurements, usually at 1-hr intervals, were hand-scaled from each magnetogram using a gauge (a ruler) etched onto a piece of glass. Calibration factors were applied to obtain physically meaningful magnetic field values (typically, horizontal intensity H, declination D, and vertical intensity Z). These data were often reported in published books, sometimes with reproductions of magnetograms recording prominent magnetic storms. Generally, the accuracy and continuity of 1-hr analog data collected after the IGY are comparable to that of modern digital data.

For many of the most intense pre-IGY storms, either few (or no) low-latitude observatories were in operation at the time, or magnetograms collected at observatories have data gaps, usually near the time of maximum disturbance. In 1921, no observatory was in operation in South Africa. At the HON observatory (Hazard, 1924a) and the Puerto Rico observatory (Vieques, VQS, the predecessor to SJG; Hazard, 1925), the magnetometers were not set up to record the wide variational range of the May 1921 storm; the H-component light traces went off the edge of the photographic paper, resulting in long data gaps of 13 and 32 hr, respectively. The KAK record has a 2-hr gap at about the time of storm maximum intensity (Kunitomi, 1921).

3. Measures of Midlatitude Geomagnetic Activity

Incompleteness also affects magnetogram records from many midlatitude observatories for the May 1921 storm. For example, the Cheltenham (CLH, Maryland) records have numerous gaps, one of which is 40 hr in duration (Hartnell, 1921; Hazard, 1924b); the storm was incompletely recorded at Kew in London (e.g., Chree, 1921) and at Eskdalemuir (ESK) in Scotland (Mitchell, 1921), partly because the light trace went off the edge of the photographic paper and partly because the trace on the paper was too faint to be resolved on account of the extreme rapidity of geomagnetic variation.

At midlatitudes, a qualitative assessment of geomagnetic disturbance is provided by the *aa* index (e.g., Mayaud, 1980), which roughly quantifies the average range of geomagnetic activity among the three vector components over sequential 3-hr windows of time, as measured at two nearly antipodal observatories (one in the Northern Hemisphere and one in the Southern Hemisphere). In 1921, the two observatories that contributed to *aa* were Greenwich (GRW; 51.48°N, 00.00°E; geomagnetic for 1920: 54.15°S, 83.03°E) and Toolangi (TOO, 37.53°S, 145.47°E; geomagnetic: 46.52°S, 139.95°E), Australia. The *aa* index is essentially an average of dimensionalized *K*-index values (Bartels et al., 1939) from those two observatories. As such, the *aa* index is quantized, with integer values in nanotesla corresponding, approximately, to the logarithm of the typical magnetic variational range. The highest *aa* level that could be attained in May, 1921 is 680 nT, a reference value that nominally represents geomagnetic magnetic variation as realized only during the most intense storms—it does not accurately quantify great levels of localized variation, such as those seen in May 1921 when variation exceeded the dynamic range of the recording magnetometer. We note that a recent renormalization of *aa* results in a higher peak value in May 1921 of 832 nT (Lockwood et al., 2018), though this also does not represent the actual range of localized field variation. The *aa* index is continuous in time from 1868 to the present.

4. Analog Magnetogram Records for the May 1921 Storm

From inspection of observatory records held in several archives, for the May 1921 storm, we identify four complete (or reasonably complete) geomagnetic records from low-latitude magnetic observatories located at Watheroo, Australia (WAT, 30.32°S, 115.88°E; geomagnetic for 1920: 41.56°S, 175.08°E), Apia, Western Samoa (API, 13.81°S, 188.22°E; geomagnetic: 16.09°S, 100.41°E), San Fernando, Spain (SFS, 36.46°N, 353.79°E; geomagnetic: 40.89°N, 70.57°E), and Vassouras, Brazil (VSS, 22.400°S, 316.35°E; geomagnetic: 11.81°S, 23.29°E). Note: In 1921, observatories often reported data in time relative to either an identified local longitude or relative to Greenwich Mean Time (GMT); standard time zones had not yet been globally adopted (e.g., Howse, 1997). Note that, for our purposes, 00:00 GMT is essentially 00:00 Universal Time (UT).

The WAT 1919–1935 summary book (Fleming et al., 1947) contains hourly average values with time stamps centered on the middle of the hour (00:30, 01:30, etc.) for meridian 120.00°E; reproductions of selected magnetograms are given in the back of the book. The API 1921 yearbook (Westland, 1923, p. 37) contains hourly average values with time stamps centered on the middle of the GMT hour; a reproduction of a magnetogram recording the 1921 storm is available (Angenheister & Westland, 1921a). The SFS 1921 yearbook (Instituto y Observatorio de Marina, 1924, p. 145) contains hourly values and spot values in local time, approximately at the middle of the GMT hour. The SFS table of hourly values has two 1-hr data gaps of relevance, one on 13 May, hour 12, and one on 15 May, hour 5. The 14 May, hour 23 value appears to be a transcription error; instead of 276 nT, judging from prior and subsequent data values, it should actually read 976 nT.

The results reported in the VSS 1915–1923 summary book (Lemos, 1927, p. 224–225) require manipulation to be useful. Hourly values are given in local time (close to 3 hr behind GMT), but there is a long gap of 10 hr during storm main phase. Reproductions of the VSS magnetograms are given in plates in the summary book with unlabeled 1-hr marks. These have several significant abrupt offsets during storm main phase (corresponding to the gap in the table of hourly values), likely due to the placement of deflecting mirrors to ensure that the magnetometer light beam did not wander off the edge of the photographic paper. We note, furthermore, that the magnetograms in the yearbook are upside-down, and on the magnetogram for 14 May, the horizontal intensity, instead of being labeled "H," was (mistakenly) labeled "D" (as if for declination).

To fill the long gap in the VSS yearbook hourly values and obtain values with time stamps on the middle of the GMT hour (modulo 24 hr), as is (more or less) the case for the WAT, API, and SFS values, we use a vector-graphics program to make a graphical copy of the magnetograms recording horizontal-component variation. This allows us to adjust for the abrupt offsets and make the magnetogram into a continuous whole; we show a reproduction of the magnetogram in Figure 1. We can partially check the integrity of the continuous magnetogram against the hourly values (on the top of the GMT hour, modulo 24) reported in the VSS book. Then, we pick off hourly values at the middle of the GMT hour to obtain a continuous record of the storm.

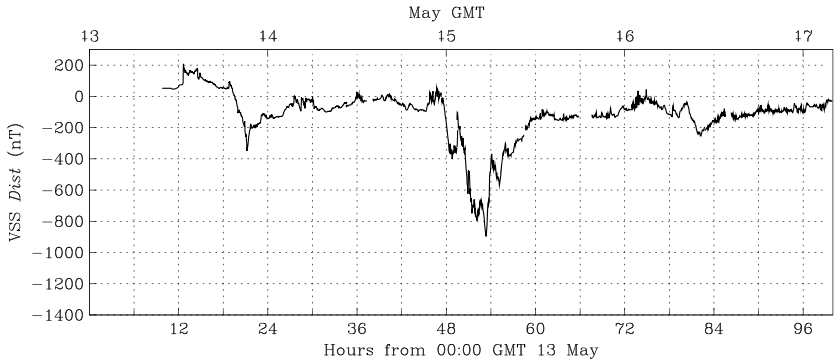

Figure 1. Time series of Vassouras (VSS) horizontal-component variation reconstructed from magnetogram fragments given in VSS yearbook.

5. Estimating May 1921 *Dst*

We use the hourly WAT, API, VSS, and SFS data values to construct a Dst_{WAVS} time series representation of the May 1921 storm. Similar to the standard calculation of *Dst* (Sugiura & Kamei, 1991), local disturbance can be defined at each observatory as

$$Dist_{\mathrm{i}}(\mathrm{t}) = H_{\mathrm{i}}(\mathrm{t}) - Sq_{\mathrm{i}}(\mathrm{t}) - C$$

(e.g., Love & Gannon, 2009), where $H_i(t)$ is 1-hr resolution variation in time t of geomagnetic horizontal intensity recorded at the ith observatory; $Sq_i(t)$ is quasi-diurnal time variation generated by tidal electric currents in the ionosphere and, to a lesser extent, in the Earth; C is a baseline representing the Earth's main field and the permanent magnetization of the crust beneath the observatory site. The Kyoto method for calculating *Dst* uses data from months of data time series to calculate C and frequency-band-limited $Sq_i(t)$. Our algorithm is simpler. We estimate $Sq_i(t)+C$ by using a pre-storm quiet day preceding storm commencement. We subtract the quiet day variation from the hourly values to obtain the local $Dist_i(t)$ time series at each observatory. Results are insensitive to the details of this reduction since $|Sq_i(t)| \ll |Dist_i(t)|$over most of the duration of the storm. Next, following the Kyoto method, we assume that geomagnetic disturbance, generated by magnetopause and ring current systems far above the Earth's surface, is spatially uniform over the dimension of the Earth and roughly aligned with the geomagnetic pole. With this, we weight each disturbance time series $Dist_i(t)$ by 1/cos λ, where λ is the geomagnetic latitude of the observatory. Upon averaging across the four observatories,

$$Dst(t) = \frac{1}{4}\sum_{i=1}^{4}\frac{Dist_{\mathrm{i}}(t)}{\cos\lambda_i},$$

we obtain the storm time disturbance time series (e.g., Love & Gannon, 2009, section 4; Mursula et al., 2008).

Before we proceed, we test our *Dst* estimation method. For the great magnetic storm of March 2001 (Gonzalez et al., 2011; Wang et al., 2004), we use our algorithm and data from API, VSS, and SFS; in place of WAT (which was no longer in operation in 2001), we use data from its nearby replacement at Gnangara, Australia (GNA, 31.78°S, 115.95°E). We show this test Dst_{GAVS} time series in Figure 2, along with the four (latitude-weighted) $Dist_i(t)/\cos\lambda_i$ time series and the official Dst_{Kyoto} the storm. Generally, agreement between the time series is very good. Over the 9-day duration of time shown, the root-mean-squared (RMS) difference between Dst_{GAVS} and Dst_{Kyoto} is 13 nT or much less than the *Dst* range of 423 nT. The maximum $-Dst_{\mathrm{GAVS}}$ value is 361 nT, which for Dst_{Kyoto} is −387 nT, a difference of 26 nT and a relative difference of about 7%. While these differences might be expected to be larger for a more intense magnetic storm, such as that of May 1921, they do satisfactorily validate our method, including our use of nonstandard stations for calculating *Dst*. In Figure 3a, we show the *Dst* time series for May 1921, along with the four (latitude-weighted) disturbance time series $Dist_i(t)/\cos\lambda_i$.

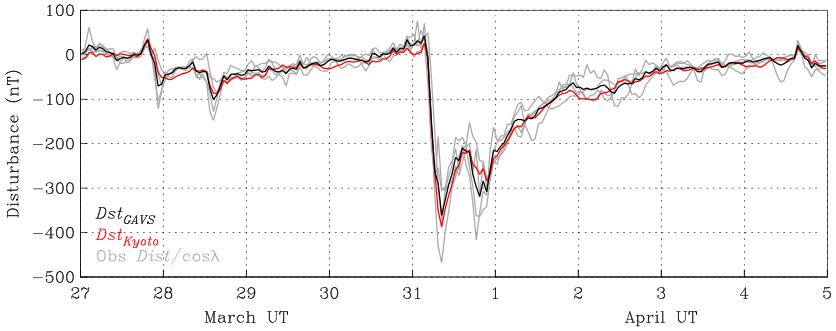

Figure 2. Our estimated Dst_{GAVS} (black) time series obtained using data from Gnangara (GNA), Apia (APi), Vassouras (VSS), and San Fernando (SFS); latitude-weighted disturbance for all four $Dist_i(t)/\cos\lambda_i$ (gray), and the official Dst_{Kyoto} (red) from 00:30 UT March 27 to 23:30 UT 5 April 2001.

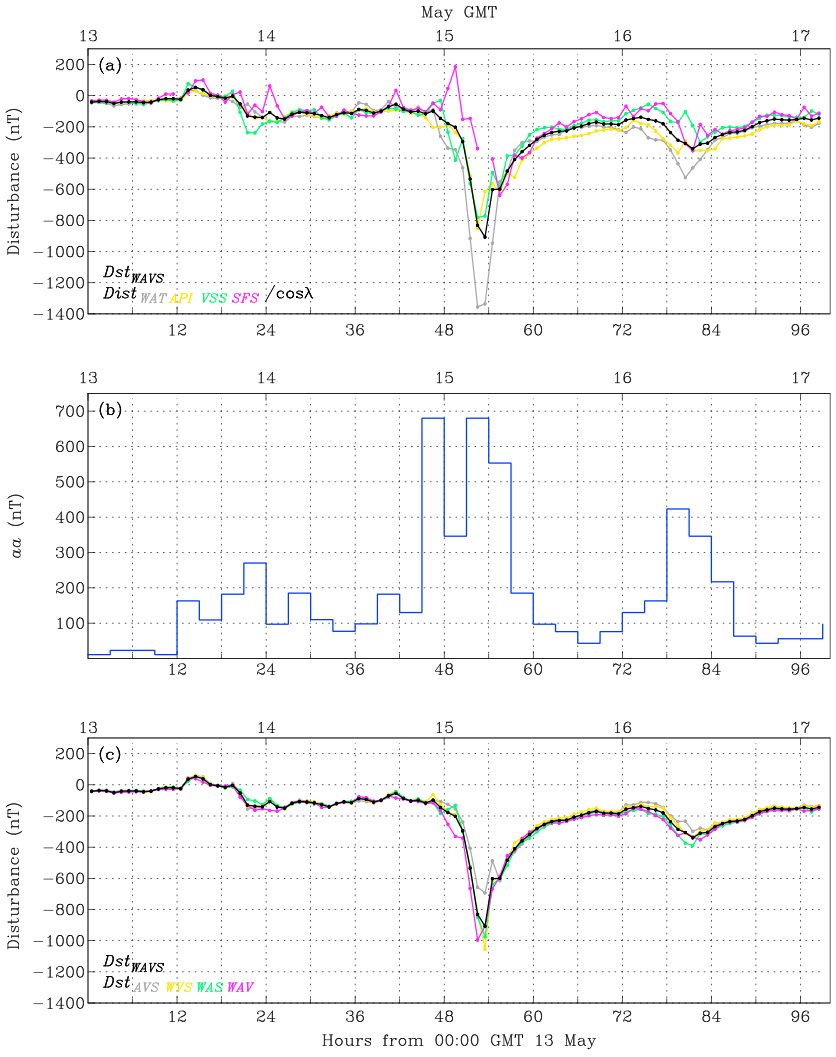

Figure 3. (a) Latitude-weighted disturbance time series from the Watheroo (WAT, gray), Apia (API, yellow), Vassouras (VSS, green), and San Fernando (SFS, purple) observatories, and the Dst_{WAVS} time series (black) from 00:30 GMT on 13 May to 02:30 GMT on 17 May 1921. Numerical values are given in a supporting file provided with this report. (b) The *aa* geomagnetic index. (c) Three-station *Dst* time series, Dst_{AVS} (gray, omitting WAT data), Dst_{WVS} (yellow, omitting API data), Dst_{WAS} (green, omitting VSS data), Dst_{WAV} (purple, omitting SFS data), and the four-station Dst_{WAVS} (black).

6. Time Sequence of Space Weather Events in May 1921

We consider, now, the sequence of events leading up to and encompassing the magnetic superstorm of May 1921. The storm occurred during the declining phase of Solar Cycle 15. The cause of the storm can plausibly be attributed to a large (max area of 1,709 microsolar hemispheres per Greenwich Observatory records), complex (e.g., Lundstedt et al., 2015), near-equatorial sunspot group (Greenwich region 933404) that was first seen on the Sun's east limb on 8 May 1921 (e.g., Cortie, 1921) and which rotated to the west limb by 19 May 1921. Hα-spectroheliograms on 11 May and subsequent days showed great activity in various regions in and about the group (Hale & Nicholson, 1925).

Region 933404 was likely responsible for the six sudden impulses registered in ground-based magnetometer measurements from 12–20 May 1921 (Newton, 1948, p. 178), but timing and size information on eruptive flares, or other flare-monitoring information, is lacking, so we cannot confidently link a specific solar eruption to any given geomagnetic impulse. However, given modern understanding, it is reasonable to assume that the impulses were caused by the arrival at Earth of the shockwave of interplanetary coronal mass ejections (e.g., Gonzalez et al., 2007; Veenadhari et al., 2012). Each shockwave compressed the magnetosphere, generating an eastward-directed magnetopause current that was manifest in observatory magnetograms as an abrupt positive perturbation in horizontal intensity. The geomagnetic disturbance period of 12–20 May can be described as a sequence of storms, each initiated by an impulse (e.g., Angenheister & Westland, 1921b).

On 12 May, the geomagnetic field was moderately disturbed. At ~13:08 GMT on 13 May, a sudden and strong geomagnetic impulse was recorded in magnetograms from Alibag, India (~130 nT; Chinmayanandam, 1921), WAT (~70 nT; Parkinson, 1921), API (~70 nT; Angenheister & Westland, 1921b), VSS (~126 nT; Lemos, 1921); a magnetogram for 13 May is not given in the SFS yearbook. From these data, we obtain a latitude-weighted average of ~107 nT, as a measure of the size of the impulse—only seen in about 1% of all storm sudden commencements (e.g., Araki, 2014). Using an empirical relationship (e.g., Siscoe et al., 1968, equation 2; Burton et al., 1975, equation 2), we estimate the solar wind dynamic pressure at the moment of maximum magnetopause compression to be ~64.5 nPa—much higher than the quiet-time pressure of ~1.6 nPa. The subsolar magnetopause radius can be estimated from a balance of the solar wind's dynamic pressure with the pressure exerted by the Earth's magnetic field (e.g., Prölss, 2004, equation 6.75). From this, we estimate that this sudden commencement compressed the magnetopause radius from its normal quiet-time value of ~9.8 Earth radii to a subgeosynchronous value of ~5.3 Earth radii.

Following the 13 May impulse, the storm exhibited a ~6-hr initial phase during which time *Dst* was positive (Figure 3a), and *aa* indicates midlatitude disturbance (Figure 3b). Such an initial phase is normally caused by persistent solar wind pressure maintaining an eastward magnetopause current. During this time, *Dst* reached a maximum value of 111 nT at 14:30 GMT. Next came a ~16 hr decrease in *Dst*, characteristic of the "main phase" of a magnetic storm. Under conventional interpretations, southward-pointing interplanetary magnetic field connected with the magnetospheric field (Cowley, 1995; Dungey, 1961), bringing a period of magnetospheric convection, during which solar wind dragged field lines from the dayside of the magnetosphere, across the polar cap, and into the magnetotail (e.g., Kennel, 1995). Intermittent substorm collapses of the tail current and diversion of current onto Earth-directed field lines (e.g., Kamide et al., 1998; McPherron, 1997; Nishida, 1978) contributed to local time asymmetry in low-latitude ground-level geomagnetic disturbance, such as seen at ~22:30 GMT on 13 May in Figure 3a. Injections of ions into the equatorial ring current (e.g., Kozyra & Liemohn, 2003) brought amplification of the ring current and an increase in $-Dst$ to a maximum of 149 nT. By ~20:30 GMT on 14 May, this first initial stormy period had largely dissipated.

A second, more intense, stormy period began with the arrival of another impulse at 22:13 GMT on 14 May (Angenheister & Westland, 1921b). Extreme asymmetry in low-latitude geomagnetic disturbance followed, notably from about 00:30 to 05:30 GMT on 15 May. Note that during this time, the SFS observatory, located at about local time midnight to early morning, recorded an anomalously positive disturbance of 209 nT (Figure 3a), which was likely due to substorm field-aligned, region-1 currents, connecting the magnetopause with auroral-zone ionospheric currents; similar asymmetry was realized during the early stages of the "Halloween storm" of October 2003 (e.g., Love & Gannon, 2010, Figure 6a, b). For the May 1921 storm, low-latitude asymmetry was simultaneous with pronounced midlatitude geomagnetic disturbance, with

aa reaching its peak (saturated) value of 680 nT. At its most extreme depth, the main phase of the May 1921 storm reached a maximum $-Dst$ of 907 nT at 05:30 GMT on 15 May; this hourly value is based on data from just three observatories (WAT, API, and VSS), since the SFS observatory has a 1-hr gap at about 05:30 GMT.

Even at maximum $-Dst$, low-latitude geomagnetic disturbance was extremely asymmetric and midlatitude disturbance pronounced. The hourly average latitude-weighted disturbance, $Dist/\cos\lambda$, at the WAT observatory attained 1,355 nT at 04:30 GMT on 15 May; the latitude-weighted instantaneous (not hourly average) local disturbance at WAT attained a value of 1,438 nT at 04:21 GMT (Fleming et al., 1947, p. 459). This latter value is tremendous, and we only know it to have been exceeded by the 1,760 nT value recorded in instantaneous measurements from the Colaba (CLA), India observatory during the Carrington event of 1859 (e.g., Tsurutani et al., 2003); note that the −1,760 nT Colaba value is not an hourly average value but a spot value (e.g.,Gonzalez et al., 2011; Siscoe et al., 2006) and so should be compared to the 1,438 nT WAT value and not the hourly average value 1,355 nT. By 16 May, this intense stormy period had dissipated, only to be followed by yet another impulse on 16 May and another stormy period.

We estimate the error associated with the 1-hr gap in the SFS record at what is apparently storm $-Dst$ maximum at 05:30 GMT on 15 May by calculating four separate three-station *Dst* time series, which we compare in Figure 3c to our best estimate of *Dst*, denoted as Dst_{WAVS}, obtained using all the available data (accommodating the SFS gap) from all four stations. At 04:30 GMT on 15 May, or 1 hr immediately prior to storm maximum, the range in three-station $-Dst$ is given by $-Dst_{\mathrm{WAV}} = 996$ nT, obtained using data from WAT, API, and VSS (omitting data from SFS), and $-Dst_{\mathrm{AVS}} = 657$ nT, obtained using data from API, VSS, and SFS (omitting data from WAT), for an absolute difference of 338 nT. Dividing the range in half (169 nT) and then dividing by the four-station $-Dst_{\mathrm{WAVS}} = 832$ nT, we obtain a relative range error of 20% for one missing station. The RMS difference between the three-station estimates and the four-station estimates at 04:30 is 120 nT, corresponding to a relative difference of 14%. Though the three-station estimates are not statistical nor independent, the RMS value is something similar to common notions of error. With it, our best estimate of storm maximum $-Dst = 907$ nT has an uncertainty of ± 132 nT.

7. Timeline and Geography of Impacts

The May 1921 magnetic storm brought interference to over-the-horizon radio communication, including static and variable reception signal strength (The New York Times, 15 May 1921, p. 1; Gibbs, 1921), but most reports of impact were to landline telephone and telegraph systems (e.g., The New York Times, 26 May 1921, p. 18). Early interference to telegraph systems came at 14:30 Pacific local time (no daylight savings time; 22:30 GMT) on 13 May (The Los Angeles Times, 15 May 1921, pp. 1–2), corresponding to the main phase of the first stormy period recorded by *Dst* in Figure 3a and the midlatitude disturbance recorded in *aa* in Figure 3b. Storm-related effects were particularly pronounced across the eastern United States, where fluctuating electric currents grew to a level where "hardly a wire was working anywhere," and "Earth currents" affected underground wires (The New York Times, 15 May 1921, p. 1). Over the next couple of days, fuses were blown on telegraph systems (The Boston Globe, 16 May 1921, p. 14), and stray voltages on some wires exceeded 1,000 V (The Washington [D.C.] Sunday Star, 15 May 1921, p. 1; The New York Times, 17 May 1921, p. 1). During the nights of 14–15 May, aurorae were seen in many nighttime skies, in both Northern and Southern hemispheres, and, in some cases, down to magnetic latitudes of ~16° (per Kyoto World Data Center calculator for 1920 main field model; Angenheister & Westland, 1921a; Silverman & Cliver, 2001).

Storm-related effects were especially acute in New York City and across New York State. Between early morning and afternoon, local time (afternoon or evening GMT), on 14 May, possibly at about the time of the sudden impulse at 22:13 GMT on 14 May, excessive electric currents on telephone lines caused the Union Railroad Station in Albany, New York, to catch fire; the station burned to the ground, and a "great many" Bell System cables were damaged (Telephone Review, 12, 1921, p. 130). In the evening of 14 May (early morning GMT on 15 May), during main phase development of the second (and most intense) stormy period, when substorm disturbance could be expected to drive localized geomagnetic disturbance at midzone and auroral-zone latitudes, a telegraph operator, working at the Central New England Railroad station in the village of Brewster (north of New York City), was driven from his keys by "electric fluid" that suddenly "flared out," igniting the switchboard and setting the station building afire (The Bridgeport Telegram, 17

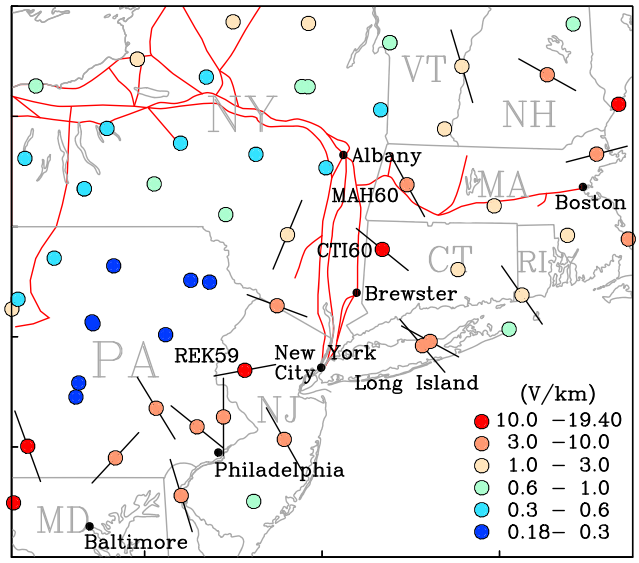

Figure 4. Map of the northeast United States centered on the New York City area and upstate New York showing 100-year geoelectric field amplitude and most likely geoelectric field polarization (for sites with amplitude greater than 3.0 V/km). Also shown (red) are the principal railroad lines uses by the New York Central Railroad (Poor & Poor, 1920, p. 759).

May 1921, p. 11). Meanwhile, aurorae over New York City were apparently so bright that even "the intense lights of the electric signs along Broadway could not dim the brilliance of the flaring skies" (The New York Times, 15 May, p. 1).

At about 01:00 local time (with daylight savings time, 05:00 GMT) on 15 May, close in time to the extreme depth of the storm, numerous telephone lines connecting Brooklyn (New York City) to Long Island (New York State) went out of service as heat coils and arrestors blew out (Telephone Review, 12, 1921, p. 130). At 07:04 local time (11:04 GMT), on 15 May, during storm recovery, the New York Central Railroad was abruptly brought to a halt below 125th Street (New York City) when the signal and switching system was put out of operation; this was followed by a fire in the control tower at 57th Street and Park Avenue (New York Times, 16 May 1921, p. 2). In a recent review of the effects of the May 1921 storm, Hapgood (2019) has questioned whether or not this particular event (disruption of the New York Central Railroad) was actually related to the storm, especially since it was reported to have occurred after storm maximum when local geomagnetic intensity was probably more subdued than during storm main phase; Hapgood raises good points, but we remain impressed with reports of "ground currents" in and around New York City exceeding 1000 volts—these would, more certainly, have caused "mischief" to signaling systems of the New York Central Railroad (New York Times, 17 May 1921, pp. 1 and 4).

The causal connection between storm time geomagnetic disturbance and its impact on electricity networks, communication landlines, and pipelines has been qualitatively understood for years (e.g., Boteler, 2001; Pirjola, 2002; Pulkkinen et al., 2017; Thomson et al., 2009). Time-dependent geomagnetic field variation can induce geoelectric fields in the Earth's conducting interior, and these fields, in turn, can drive quasi-direct currents through grounding connections of electrically conducting networks. Recent integrations have brought this theory into quantitative focus. Three separate factors are important (e.g., Blake et al., 2016; Lucas et al., 2018; Mac Manus et al., 2017; Marshall et al., 2019; Torta et al., 2017): (1) the localized details of geomagnetic vector disturbance responsible for the induction in the Earth, (2) the geographic expression of the Earth's surface impedance tensor, giving the frequency dependent relationship between the inducing geomagnetic disturbance and the induced geoelectric field, and (3) the topology of the conducting network, since geomagnetically induced voltage is determined by the integrated projection of the geoelectric field onto line segments connecting grounding points. A conspiracy of these factors together allowed the magnetic storm of May 1921 to adversely impact the telephone and telegraph networks of New York, some of which were either colocated with or used to support the operation of train systems. To calculate geomagnetically induced currents, the connectivity of the network and its electrical resistivity properties are needed.

For geographic perspective, in Figure 4, we show a geoelectric field hazard map—amplitudes of horizontal-component geoelectric field, as would be expected to be exceeded during magnetic storms only once per century (on average) and corresponding polarizations, extracted from results given by Love, Lucas, et al. (2019). This map was constructed by analyzing geoelectric field time series obtained by convolving long 1-min resolution digital geomagnetic field time series acquired at modern observatories, operated by the U.S. Geological Survey (Love & Finn, 2011) and Natural Resources Canada (Newitt & Coles, 2007), with impedance tensors acquired as part of a national-scale magnetotelluric survey supported by the National Science Foundation (Schultz et al., 2006, 2010). The geoelectric time series at each survey site were then analyzed for extreme values and statistically extrapolated to 100-year values. As such, Figure 4 amounts to a summary of factors (1) and (2) affecting the induction-related impacts across the New York region and the broader northeast United States.

As Love, Lucas, et al. (2019) have noted, the high-geoelectric hazards shown in Figure 4 are part of a band running from the southwest to the northeast that more or less corresponds to igneous and metamorphic rock

of the (highly eroded) Appalachian Mountains and the New England Highlands. Such rock types tend to be relatively electrically resistive, corresponding to high impedance, and, thus, for a given level of geomagnetic disturbance, geoelectric hazards will tend to be high. In contrast, low-geoelectric hazards are seen to the northwest, across the sedimentary rocks of Appalachian Plateau. Such rock types tend to be relatively electrically conductive, corresponding to low impedance and, for a given level of geomagnetic disturbance, lower geoelectric hazards. Notably, geoelectric hazards are relatively high around New York City and southeast New York State (NY).

Turning, now, to factor (3), in Figure 4, we show a map of the principal railroad lines used by the New York Central Railroad in 1921. Recall that the railway station in Albany was set afire by excessive current on telephone lines. We do not know the orientation of the specific telephone line (or lines) that caused the fire, but one line could have plausibly run along the primary railroad line in western Massachusetts (MA, west of Boston) and have connected to the Albany station. We note survey site MAH60 (42.38°N, −73.04°E) has a polarization of −34.36°, which is almost parallel to the direction of the nearby railroad line. Assuming that the May 1921 storm generated a geoelectric field with an amplitude like the 100-year amplitude estimated for this site, or 7.69 V/km, then the integrated voltage on a telephone line, with (say) 100 km between grounding points, would have equaled about 769 V. This specific value is speculative, of course, but we can safely infer that the "1,000 volts" reported on some telegraph lines during the May 1921 storm could have actually been realized.

Further to this point, we note that the survey site CTI60 in western Connecticut (CT, 41.79°N, −73.32°E) is located just 27 km north of the village of Brewster (41.40°N, −73.62°E), where the railroad station burned down, in this case, due to overheating telegraph systems. At CTI60, the once per century geoelectric field is 19.40 V/km. Assuming that a geoelectric field of similar amplitude was generated during the May 1921 storm, then for an optimally oriented telegraph line, with 100 km between grounding points, the integrated voltage would have been about 1,940 V, or much more than the "1,000 V" reported on some telegraph lines during the May 1921 storm. To the west of New York City is survey site REK59 in New Jersey (NJ, 40.70°N, −74.87°E); here the 100-year amplitude is 12.98 V/km, again, sufficient to induce voltages in excess of "1,000 V" on telephone and telegraph lines.

8. Context and Conclusions

Today, it is recognized that numerous technological systems are potentially vulnerable to the impacts of intense magnetic storms. They are associated with damage to satellite electronics and increased orbital drag, disruption to over-the-horizon radio communication, degradation in the accuracy and reliability of global-positioning and timing systems, interference with geophysical surveys, increased radiation exposure to astronauts and high-altitude pilots, and the induction of currents in electric-power grids that sometimes cause blackouts (e.g., Daglis, 2004; Hapgood, 2018b). The most intense magnetic storm since the IGY (1957–1958), that of March 1989 (Allen et al., 1989), had a maximum $-Dst = 589$ nT. This storm is especially notable because it caused an electricity blackout in Québec, Canada. This impact on electricity power grids is essentially the modern version of the disturbance summarized here for landline telegraph and telephone systems in May 1921. Indeed, should a storm as intense as that of May 1921 occur today, its impact on electricity networks might exceed that realized in March 1989.

While intense storms, such as that of May 1921, generally exhibit magnetic disturbance across all latitudes, it is important to recognize that the *Dst* index is only a measure of low-latitude disturbance as generated by the symmetric part of the magnetospheric ring current. Here we have interpreted local time asymmetry in the low-latitude disturbance time series, the WAT, API, VSS, and SFS magnetometer data that we used to estimate *Dst*, as a plausible indication of higher-latitude disturbance (such as across New York State). This is a conventional, if limited, method of interpretation. With midzone and auroral-zone magnetometer data, more detailed analyses can be made of storm time field-aligned and auroral-zone current systems.

If geomagnetically induced currents are to be understood and modeled to the point of enabling, for example, accurate predictions, then we certainly need regional maps of geomagnetic disturbance, regional maps of surface impedance, and the power-grid system configurations and physical parameters (e.g., Love et al., 2018). Lacking parts of these causally connected information sets, some studies have focused on empirically derived correlations (applicable for particular system configurations and parameters), such as those that can

be established between local measured geomagnetic disturbance and measured grid currents (e.g., Clilverd et al., 2018; Pulkkinen et al., 2001). Hazard analyses would benefit from a quantification of the spatio-temporal relationship between global geomagnetic disturbance, such as measured by *Dst*, and localized geomagnetic disturbance. With that, historical *Dst* time series, such as that developed here, could be more completely exploited for practical applications.

Acknowledgments
We thank A. Kelbert, K. A. Lewis, J. McCarthy, J. L. Slate, and two anonymous reviewers for reading a draft manuscript. This work was supported by the Geomagnetism Program of the U.S. Geological Survey; H. Hayakawa is supported by a fellowship (JP17J06954) and a Grant in Aid (JP15H05816) from the Japanese Society for the Promotion of Science. Royal Observatory, Greenwich-USAF/NOAA sunspot data are available online (https://solarscience.msfc.nasa.gov/greenwch.shtml). We provide numerical values of observatory disturbance and *Dst* in the supporting information provided with this report. Standard *Dst* index values are provided by the Kyoto World Data Center in Japan (wdc.kugi.kyoto-u.ac.jp). Standard *aa* values are provided by the Service International des Indices Géomagnétiques (http://isgi.unistra.fr) and the British Geological Survey (www.geomag.bgs.ac.uk). Regarding the books used in this analysis, the WAT book is widely available. The API book is somewhat rare; we used a copy obtained from Geology and Nuclear Science (GNS), New Zealand. The VSS book was obtained from the Kyoto World Data Center. The SFS book was obtained from the Linda Hall Library in Kansas City, MO. Copies of some observatory yearbooks for 1921 and various editions of Poor's Manual of Railroads are available through the Hathi Trust. The New York Times has a searchable archive of historical articles available online (https://www.nytimes.com/search/), as does the Washington Post (http://www.washingtonpost.com/wp-adv/front.htm); for Australia (trove.nla.gov.au); for France (gallica.bnf.fr); commercial archives such as Newspapers.com can also be used. Any use of trade, firm, or product names is for descriptive purposes only and does not imply endorsement by the U.S. Government.

References

Allen, J., Frank, L., Sauer, H., & Reiff, P. (1989). Effects of the March 1989 solar activity. *Eos, Transactions American Geophysical Union*, *70*(46), 1479, 1486-1488. https://doi.org/10.1029/89EO00409

Angenheister, G., & Westland, C. J. (1921a). The magnetic storm of May 13-14, 1921a: Observations at Samoa Observatory. *New Zealand Journal of Science and Technology*, *4*(4), 201–202.

Angenheister, G., & Westland, C. J. (1921b). The magnetic storm of May 13-16, 1921b, at Apia Observatory, Samoa. *Terrestrial Magnetism and Atmospheric Electricity*, *26*(1-2), 30–31. https://doi.org/10.1029/TE026i001p00030

Araki, T. (2014). Historically largest geomagnetic sudden commencement (SC) since 1868. *Earth Planets Space*, *55*(1), 164. https://doi.org/10.1186/s40623-014-0164-0

Baker, D. N., Balstad, R., Bodeau, J. M., Cameron, E., Fennell, J. F., Fisher, G. M., et al. (2008). *Severe space weather events—Understanding societal and economic impacts* (pp. 1–144). Washington, DC: The National Academy Press.

Bartels, J., Heck, N. H., & Johnston, H. F. (1939). The three-hour range index measuring geomagnetic activity. *Terrestrial Magnetism and Atmospheric Electricity*, *44*(4), 411–454. https://doi.org/10.1029/TE044i004p00411

Blake, S. P., Gallagher, P. T., McCauley, J., Jones, A. G., Hogg, C., Campanya, J., et al. (2016). Geomagnetically induced currents in the Irish power network during geomagnetic storms. *Space Weather*, *14*, 1154. https://doi.org/10.1002/2016SW001534

Boteler, D. H. (2001). Space weather effects on power systems. In P. Song, H. J. Singer, & G. L. Siscoe (Eds.), Geophys. Monog. 125*Space weather* (pp. 347–352). Washington, DC: American Geophysical Union. https://doi.org/10.1029/GM125p0347

Burton, R. K., McPherron, R. L., & Russell, C. T. (1975). An empirical relationship between interplanetary conditions and *Dst*. *J. Geophys. Res.*, *80*(31), 4204–4214. https://doi.org/10.1029/JA080i031p04204

Cannon, P., Angling M., Barclay, L., Curry, C., Dyer, C., Edwards, R., et al. (2013). Extreme space weather: Impacts on engineered systems and infrastructure (pp. 1-68). London, UK: Royal Academy of Engineering.

Chinmayanandam, T. K. (1921). The magnetic storm of May 13-17, 1921, at Alibag Observatory, India. *Terrestrial Magnetism and Atmospheric Electricity*, *26*(1-2), 28–29. https://doi.org/10.1029/TE026i001p00028

Chree, C. (1921). The magnetic storm of May 13-17. *Nature*, *107*(2690), 359. https://doi.org/10.1038/107359a0

Clilverd, M. A., Rodger, C. J., Brundell, J. B., Dalzell, M., Martin, I., Mac Manus, D. H., et al. (2018). Long-lasting geomagnetically induced currents andharmonic distortion observed in New Zealand during the 7–8 September 2017 disturbed period. *Space Weather*, *16*, 704–717. https://doi.org/10.1029/2018SW001822

Cliver, E. W., & Dietrich, W. F. (2013). The 1859 space weather event revisited: Limits of extreme activity. *Journal of Space Weather and Space Climate*, *3*, 15. https://doi.org/10.1051/swsc/2013053

Cortie, A. L. (1921). The sun-spot group and the magnetic disturbances, 1921 May 8-21. *Monthly Notices of the Royal Astronomical Society*, *81*(6), 515–520. https://doi.org/10.1093/mnras/81.8.515

Cowley, S. W. H. (1995). The Earth's magnetosphere: A brief beginner's guide. *Eos, Transactions American Geophysical Union*, *76*(51), 525.

Daglis, I. A. (2001). The storm-time ring current. *Space Science Reviews*, *98*(3-4), 343–363. https://doi.org/10.1023/A:1013873329054

Daglis, I. A. (Ed.) (2004). *Effects of space weather on technology infrastructure* (pp. 1–334). Dordrecht, The Netherlands: Kluwer Academic Publishers.

Dungey, J. W. (1961). Interplanetary magnetic field and the auroral zones. *Physical Review Letters*, *6*(2), 47–48. https://doi.org/10.1103/PhysRevLett.6.47

Eastwood, J. P., Biffis, E., Hapgood, M. A., Green, L., Bisi, M. M., Bentley, R. D., et al. (2017). The economic impact of space weather: Where do we stand? *Risk Analysis*, *37*, 206–218. https://doi.org/10.1111/risa.12765

Echer, E., Gonzalez, W. D., & Tsurutani, B. T. (2011). Statistical studies of geomagnetic storms with peak Dst ≤ -50nT from 1957 to 2008. *Journal of Atmospheric and Solar-Terrestrial Physics*, *73*, 1454–1459. https://doi.org/10.1016/j.jastp.2011.04.021

Fleming, J. A., Johnston, H. F., Forbush, S. E., McNish, A. G., Scott, W., & E. (1947). *Magnetic results from Watheroo Observatory, Western Australia, 1919-1935, Volume VII-A* (pp. 1–1122). Washington, DC: Carnegie Institution of Washington.

Ganushkina, N., Jaynes, A., & Liemohn, M. (2017). Space weather effects produced by the ring current particles. *Space Science Reviews*, *212*(3-4), 1315–1344. https://doi.org/10.1007/s11214-017-0412-2

Gibbs, A. (1921). Effects of the recent aurora on telegraph-lines, telephone-lines and wireless stations. *New Zealand Journal of Science and Technology*, *4*(August), 183–188.

Gonzalez, W. D., Echer, E., Clua-Gonzalez, A. L., & Tsurutani, B. T. (2007). Interplanetary origin of intense geomagnetic storms (Dst < -100 nT) during solar cycle 23. *Geophysical Research Letters*, *34*, L06101. https://doi.org/10.1029/2006GL028879

Gonzalez, W. D., Echer, E., Tsurutani, B. T., Clúa de Gonzalez, A. L., & Dal Lago, A. (2011). Interplanetary origin of intense, superintense and extreme geomagnetic storms. *Space Science Reviews*, *158*(1), 69–89. https://doi.org/10.1007/s11214-010-9715-2

Gonzalez, W. D., Joselyn, J. A., Kamide, Y., Kroehl, H. W., Rostoker, G., Tsurutani, B. T., & Vasyliunas, V. M. (1994). What is a geomagnetic storm? *Journal of Geophysical Research*, *99*(A4), 5771–5792. https://doi.org/10.1029/93JA02867

Hale, G. E., & Nicholson, S. B. (1925). The law of sun-spot polarity. *Astrophysical Journal*, *62*(11), 270–300. https://doi.org/10.1086/142933

Hapgood, M. (2018a). Space weather: What are policymakers seeking. In N. Buzulukova (Ed.), Chapter 27*Extreme space weather: Origins, predictability, and consequences* (pp. 657–682). Amsterdam, The Netherlands: Elsevier.

Hapgood, M. (2018b). Linking space weather science to impacts—The view from Earth. In N. Buzulukova (Ed.), Chapter 1*Extreme space weather: Origins, predictability, and consequences* (pp. 3–34). Amsterdam, The Netherlands: Elsevier.

Hapgood, M. (2019). The great storm of May 1921: An example of a dangerous space weather event. *Space Weather*. https://doi.org/10.1029/2019SW002195

Hartnell, G. (1921). The magnetic storm of May 13–16, 1921, at Cheltenham Observatory, Maryland. *Terrestrial Magnetism and Atmospheric Electricity*, *26*(1-2), 25–25. https://doi.org/10.1029/TE026i001p00025-02

Hayakawa, H., Ebihara, Y., Hand, D. P., Hayakawa, S., Kumar, S., Mukherjee, S., & Veenadhari, B. (2018). Low-latitude aurorae during the extreme space weather events in 1859. *Astrophysical Journal*, *869*(1), 57. https://doi.org/10.3847/1538-4357/aae47c

Hayakawa, H., Ebihara, Y., Willis, D. M., Hattori, K., Giunta, A. S., Wild, M. N., et al. (2018). The great space weather event during 1872 February recorded in East Asia. *Astrophysical Journal*, *862*(1), 15. https://doi.org/10.3847/1538-4357/aaca40

Hayakawa, H., Mitsuma, Y., Fujiwara, Y., Kawamura, A. D., Kataoka, R., Ebihara, Y., et al. (2017). The earliest drawings of datable auroras and a two-tail comet from the Syriac Chronicle of Zūqnīn. *Publications of the Astronomical Society of Japan*, *69*, 17(2). https://doi.org/10.1093/pasj/psw128

Hayakawa, H., Tamazawa, H., Uchiyama, Y., Ebihara, Y., Miyahara, H., & Kosaka, S. (2017). Historical auroras in the 990 s: Evidence of great magnetic storms. *Solar Physics*, *292*(1), 1–12. https://doi.org/10.1007/s11207-016-1039-2

Hazard, D. L. (1924a). Results of observations made at the United States coast and geodetic survey magnetic observatory near Honolulu, Hawaii in 1921 and 1922 (pp. 1-100). Washington, DC: Department of Commerce, Government Printing Office.

Hazard, D. L. (1924b). Results of observations made at the United States coast and geodetic survey magnetic observatory at Cheltenham, MS., in 1921 and 1922 (pp. 1-96). Washington, DC: Department of Commerce, Government Printing Office.

Hazard, D. L. (1925). Results of observations made at the United States coast and geodetic survey magnetic observatory at Vieques, P. R., in 1921 and 1922 (pp. 1-98). Washington, DC: Department of Commerce, Government Printing Office.

Howse, D. (1997). *Greenwich time and longitude* (pp. 1–208). London, UK: Philip Wilson Publishers.

Instituto y Observatorio de Marina (1924). Anales del Instituto y Observatorio de Marina de San Fernando, Seccion 2, Observaciones Meteorológicas, Magnéticas y Sísmicas, Año 1921 (pp. 1-166). San Fernando: Sección Tipográfica del Observatorio.

Jonas, S., Fronczyk, K., & Pratt, L. M. (2018). A framework to understand extreme space weather event probability. *Risk Analysis*, *38*(8), 1534–1540. https://doi.org/10.1111/risa.12981

Kamide, Y., Baumjohann, W., Daglis, I. A., Gonzalez, W. D., Grande, M., Joselyn, J. A., et al. (1998). Current understanding of magnetic storms: Storm-substorm relationships. *Journal of Geophysical Research*, *103*(A8), 17,705–17,728. https://doi.org/10.1029/98JA01426

Kappenman, J. G. (2006). Great geomagnetic storms and extreme impulsive geomagnetic field disturbance events—An analysis of observational evidence including the great storm of May 1921. *Advances in Space Research*, *38*(2), 188–199. https://doi.org/10.1016/j.asr.2005.08.055

Kennel, C. F. (1995). *Convection and substorms: Paradigms of magnetospheric phenomenology*. Oxford, UK: Oxford University Press.

Kotzé, P. (2018). Hermanus magnetic observatory: A historical perspective of geomagnetism in southern Africa. *History of Geo- and Space Sciences*, *9*(2), 125–131. https://doi.org/10.5194/hgss-9-125-2018

Kozyra, J. U., & Liemohn, M. W. (2003). Ring current energy input and decay. *Space Science Reviews*, *109*(1-4), 105–131. https://doi.org/10.1023/B:SPAC.0000007516.10433.ad

Kunitomi, S.-I. (1921). The magnetic storm of May 13-17, 1921 as observed at the Kakioka Magnetic Observatory. *Journal of the Meteorological Society of Japan. Ser. I*, *40*(7), 3–6. https://doi.org/10.2151/jmsj1882.40.7_en3

Lakhina, G. S., & Tsurutani, B. T. (2018). Supergeomagnetic storms: Past, present, and future. In N. Buzulukova (Ed.), Chapter 8*Extreme space weather: Origins, predictability, and consequences* (pp. 157–186). Amsterdam, The Netherlands: Elsevier.

Lemos, A. (1921). The magnetic storms of March 22–25, 1920, and May 13–17, 1921, at Vassouras Magnetic Observatory, Brazil. *Terrestrial Magnetism and Atmospheric Electricity*, *26*(3), 96–98. https://doi.org/10.1029/TE026i003p00096

Lemos, A. C. (1927). Resultado Das Observações Realizadas no Observatorio Magnetico de Vassouras 1915 a 1923, pp. 1-359, Supplemento, Observaotrio Nacional do Rio de Janeiro, Miniterio da Agricultura Industria e Commercio, Rio de Janeiro, Brazil.

Lockwood, M., Finch, I. D., Chambodut, A., Barnard, L. A., Owens, M. J., & Clarke, E. (2018). A homogeneous *aa* index: 2. Hemispheric asymmetries and the equinoctial variation. *Journal of Space Weather and Space Climate*, *8*, A58. https://doi.org/10.1051/swsc/2018044

Loewe, C. A., & Prölss, G. W. (1997). Classification and mean behavior of magnetic storms. *Journal of Geophysical Research*, *102*(7), 14,209–14,213. https://doi.org/10.1029/96JA04020

Love, J. J. (2008). Magnetic monitoring of Earth and space. *Physics Today*, *61*(2), 31–37. https://doi.org/10.1063/1.2883907

Love, J. J. (2018). The electric storm of November 1882. *Space Weather*, *16*, 37–46. https://doi.org/10.1002/2017SW001795

Love, J. J., & Chulliat, A. (2013). An international network of magnetic observatories. *Eos, Transactions American Geophysical Union*, *94*(42), 373–384. https://doi.org/10.1002/2013EO420001

Love, J. J., & Finn, C. A. (2011). The USGS Geomagnetism Program and its role in space weather monitoring. *Space Weather*, *9*, S07001. https://doi.org/10.1029/2011SW000684

Love, J. J., & Gannon, J. L. (2009). Revised Dst and the epicycles of magnetic disturbance: 1958-2007. *Annales Geophysicae*, *27*(8), 3101–3131. https://doi.org/10.5194/angeo-27-3101-2009

Love, J. J., & Gannon, J. L. (2010). Movie-maps of low-latitude magnetic storm disturbance. *Space Weather*, *8*, S06001. https://doi.org/10.1029/2009SW000518

Love, J. J., Hayakawa, H., & Cliver, E. W. (2019). On the intensity of the magnetic superstorm of September 1909. *Space Weather*, *17*, 37–45. https://doi.org/10.1029/2018SW002079

Love, J. J., Lucas, G., Bedrosian, P. A., & Kelbert, A. (2019). Extreme-value geoelectric amplitude and polarization across the Northeast United States. *Space Weather*, *17*, 379–395. https://doi.org/10.1029/2018SW002068

Love, J. J., Rigler, E. J., Kelbert, A., Finn, C. A., Bedrosian, P. A., & Balch, C. C. (2018). On the feasibility of real-time mapping of the geoelectric field across North America, USGS Open-File Report, 2018-1043 (16 p.). https://doi.org/10.3133/ofr20181043

Love, J. J., Rigler, E. J., Pulkkinen, A., & Riley, P. (2015). On the lognormality of historical magnetic storm intensity statistics: Implications for extreme-event probabilities. *Geophysical Research Letters*, *42*, 6544–6553. https://doi.org/10.1002/2015GL064842

Lucas, G. M., Love, J. J., & Kelbert, A. (2018). Calculation of voltages in electric power transmission lines during historic geomagnetic storms: An investigation using realistic Earth impedances. *Space Weather*, *16*, 185–195. https://doi.org/10.1002/2017SW001779

Lundstedt, H., Persson, T., & Andersson, V. (2015). The extreme solar storm of May 1921: observations and a complex topological model. *Annales Geophysicae*, *33*(1), 109–116. https://doi.org/10.5194/angeo-33-109-2015

Mac Manus, D. H., Rodger, C. J., Dalzell, M., Thomson, A. W. P., Clilverd, M. A., Petersen, T., et al. (2017). Long-term geomagnetically induced current observations in New Zealand: Earth return corrections and geomagnetic field driver. *Space Weather*, *15*, 1020–1038. https://doi.org/10.1002/2017SW001635

Marshall, R. A., Wang, L., Paskos, G. A., Olivares-Pulido, G., Van Der Walt, T., Ong, C., et al. (2019). Modelling geomagnetically induced currents in Australian power networks using different conductivity models. *Space Weather*, *17*, 756. https://doi.org/10.1029/2018SW002047

Mayaud, P. N. (1980). Derivation, meaning, and use of geomagnetic indices, Geophysical Monograph 22 (pp. 1-154). Washington, DC: American Geophysical Union.

McPherron, R. L. (1995). Magnetospheric dynamics. In C. T. Russell & M. G. Kivelson (Eds.), *Introduction to space physics* (pp. 400–458). Cambridge, UK: Cambridge University Press.
McPherron, R. L. (1997). The role of substorms in the generation of magnetic storms. In B. T. Tsurutani, W. D. Gonzalez, Y. Kamide, & J. K. Arballo (Eds.), *Magnetic storms, Geophysical Monograph Series* (Vol. 98, pp. 131–147). Washington, DC: American Geophysical Union.
Minamoto, Y. (2013). Availability and Access to Data from Kakioka Magnetic Observatory, Japan. *Data Science Journal*, *12*, G30–G35. https://doi.org/10.2481/dsj.G-040
Mitchell, A. C. (1921). The magnetic storm of May 13-17. *Nature*, *107*(2690), 392–393. https://doi.org/10.1038/107392c0
Mursula, K., Holappa, L., & Karinen, A. (2008). Correct normalization of the *Dst* index. *Astrophysics and Space Sciences Transactions*, *4*(2), 41–45. https://doi.org/10.5194/astra-4-41-2008
National Science and Technology Council (2015). National Space Weather Strategy (pp. 1-15). Washington, DC: Executive Office.
National Science and Technology Council (2019). National Space Weather Strategy and Action Plan (pp. 1-13). Washington, DC: Executive Office.
Newitt, L. R. (2007). Observatories, automation. In D. Gubbins & E. Herrero-Bervera (Eds.), *Encyclopedia of geomagnetism and paleomagnetism* (pp. 713–715). Dordrecht, The Netherlands: Springer.
Newitt, L. R., & Coles, R. (2007). Observatories in Canada. In D. Gubbins & E. Herrero-Bervera (Eds.), *Encyclopedia of geomagnetism and paleomagnetism* (pp. 726–727). Dordrecht, The Netherlands: Springer.
Newton, H. W. (1948). "Sudden commencements" in the Greenwich magnetic records (1879–1944) and related sunspot data. *Geophysical Supplements to the Monthly Notices of the Royal Astronomical Society*, *5*(6), 159–185. https://doi.org/10.1111/j.1365-246X.1948.tb02933.x
Nishida, A. (1978). Geomagnetic diagnosis of the magnetosphere (pp. 1-256). New York, NY: Springer-Verlag.
Parkinson, W. C. (1921). The magnetic storm of May 13–17, 1921, at Watheroo Observatory, Australia. *Terrestrial Magnetism and Atmospheric Electricity*, *26*(1-2), 26–28. https://doi.org/10.1029/TE026i001p00026-02
Pirjola, R. (2002). Review on the calculation of surface electric and magnetic fields and of geomagnetically induced currents in ground-based technological systems. *Surveys in Geophysics*, *23*(1), 71–90. https://doi.org/10.1023/A:1014816009303
Poor, H. V., & Poor, H. W. (1920). *Poor's manual of railroads* (pp. 1–2134). New York, NY: Poor's Publishing Company.
Prölss, G. W. (2004). *Physics of the Earth's space environment* (pp. 1–513). Berlin: Springer.
Pulkkinen, A., Bernabeu, E., Thomson, A., Viljanen, A., Pirjola, R., Boteler, D., et al. (2017). Geomagnetically induced currents: Science, engineering and applications readiness. *Space Weather*, *15*, 828–856. https://doi.org/10.1002/2016SW001501
Pulkkinen, A., Viljanen, A., Pajunpää, K., & Pirjola, R. (2001). Recordings and occurrence of geomagnetically induced currents in the Finnish natural gas pipeline network. *Journal of Applied Geophysics*, *48*(4), 219–231. https://doi.org/10.1016/S0926-9851(01)00108-2
Riley, P. (2018). Statistics of extreme space weather events. In N. Buzulukova (Ed.), Chapter 5*Extreme space weather: Origins, predictability, and consequences* (pp. 115–138). Amsterdam, The Netherlands: Elsevier.
Riswadkar, A. V., & Dobbins, B. (2010). *Solar storms: Protecting your operations against the Sun's 'dark side'*. Zurich Services Corporation.
Schieb, P.-A., & Gibson, A. (2011). Geomagnetic storms, Central technologies on behalf of the U.S. Department of Homeland Security. https://www.oecd.org/gov/risk/46891645.pdf
Schrijver, C. J., Kauristie, K., Aylward, A. D., Denardini, C. M., Gibson, S. E., Glover, A., et al. (2015). Understanding space weather to shield society: A global road map for 2015-2025 commissioned by COSPAR and ILWS. *Advances in Space Research*, *55*(12), 2745–2807. https://doi.org/10.1016/j.asr.2015.03.023
Schröder, W., & Wiederkehr, K.-H. (2000). A history of the early recording of geomagnetic variations. *Journal of Atmospheric and Solar-Terrestrial Physics*, *62*(5), 323–334. https://doi.org/10.1016/S1364-6826(99)00100-5
Schultz, A. (2010). A continental scale magnetotelluric observatory and data discovery resource. *Data Science Journal*, *8*, IGY6–IGY20.
Schultz, A., Egbert, G. D., Kelbert, A., Peery, T., Clote, V., Fry, B., Erofeeva, S., and staff of the National Geoelectromagnetic Facility and their contractors (2006-2018). USArray TA magnetotelluric transfer functions. https://doi.org/10.17611/DP/EMTF/USARRAY/TA
Silverman, S. M., & Cliver, E. W. (2001). Low-latitude auroras: The magnetic storm of 14–15 May 1921. *Journal of Atmospheric and Solar-Terrestrial Physics*, *63*(5), 523–525. https://doi.org/10.1016/S1364-6826(00)00174-7
Siscoe, G. L., Crooker, N. U., & Clauer, C. R. (2006). *Dst* of the Carrington storm of 1859. *Advances in Space Research*, *38*(2), 173–179. https://doi.org/10.1016/j.asr.2005.02.102
Siscoe, G. L., Formisano, V., & Lazarus, A. J. (1968). Relation between geomagnetic sudden impulses and solar wind pressure changes—An experimental investigation. *Journal of Geophysical Research*, *73*(15), 4869–4874. https://doi.org/10.1029/JA073i015p04869
Sugiura, M. (1964). Hourly value of equatorial *Dst* for the IGY. *Ann. Int. Geophys. Year*, *35*, 9–45.
Sugiura, M., & Kamei, T. (1991). Equatorial *Dst* index 1957-1986, IAGA Bull., 40, ISGI Publication Office, Saint-Maur-des-Fossess, France.
Thomson, A. W., McKay, A. J., & Viljanen, A. (2009). A review of progress in modelling of induced geoelectric and geomagnetic fields with special regard to induced currents. *Acta Geophysica*, *57*(1), 209–219. https://doi.org/10.2478/s11600-008-0061-7
Torta, J. M., Marcuello, A., Campanyà, J., Marsal, S., Queralt, P., & Ledo, J. (2017). Improving the modeling of geomagnetically induced currents in Spain. *Space Weather*, *15*, 691–703. https://doi.org/10.1002/2017SW001628
Tsurutani, B. T., Gonzalez, W. D., Lakhina, G. S., & Alex, S. (2003). The extreme magnetic storm of 1–2 September 1859. *Journal of Geophysical Research*, *108*(A7), 1268. https://doi.org/10.1029/2002JA009504
Various (1957). *Annals of the International Geophysical Year* (pp. 207–329, Vol. IV, Parts IV-V). London, UK: Pergamon Press.
Veenadhari, B., Selvakumaran, R., Singh, R., Maurya, A. K., Gopalswamy, N., Kumar, S., & Kikuchi, T. (2012). Coronal mass ejection–driven shocks and the associated sudden commencements/sudden impulses. *Journal of Geophysical Research*, *117*, A04210. https://doi.org/10.1029/2011JA017216
Vennerstrom, S., Lefevre, L., Dumbović, M., Crosby, N., Malandraki, O., Patsou, I., et al. (2016). Extreme geomagnetic storms, 1868-2010. *Solar Physics*, *291*(5), 1447–1481. https://doi.org/10.1007/s11207-016-0897-y
Wang, Y.-M., Ye, P.-Z., & Wang, S. (2004). An interplanetary origin of great geomagnetic storms: Multiple magnetic clouds. *Chinese J. Geophys.*, *47*(3), 417–423. https://doi.org/10.1002/cjg2.502
Westland, C. J. (1923). Magnetic report for the year 1921. In W. A. G. Skinner (Ed.), Apia Observatory, Samoa. Report for 1921 (pp. 10–48). Wellington, New Zealand: New Zealand Government Printer.
Wienert, K. A. (1970). *Notes on geomagnetic observatory and survey practice* (pp. 1–217). Paris, France: United Nations Educational Scientific and Cultural Organization.
World Data Center for Geomagnetism, Kyoto, Nose, M., Iyemori, T., Sugiura, M., Kamei, T. (2015). Geomagnetic *Dst* index. https://doi.org/10.17593/14515-74000